RESEARCH BRIEF

Chronic Myelogenous Leukemia–Initiating Cells Require Polycomb Group Protein EZH2

Huafeng Xie[1], Cong Peng[1], Jialiang Huang[1,2], Bin E. Li[1], Woojin Kim[1], Elenoe C. Smith[1], Yuko Fujiwara[1], Jun Qi[3], Giulia Cheloni[4,5], Partha P. Das[1], Minh Nguyen[1], Shaoguang Li[4], James E. Bradner[3,6], and Stuart H. Orkin[1,7]

ABSTRACT Tyrosine kinase inhibitors (TKI) have revolutionized chronic myelogenous leukemia (CML) management. Disease eradication, however, is hampered by innate resistance of leukemia-initiating cells (LIC) to TKI-induced killing, which also provides the basis for subsequent emergence of TKI-resistant mutants. We report that EZH2, the catalytic subunit of Polycomb Repressive Complex 2 (PRC2), is overexpressed in CML LICs and required for colony formation and survival and cell-cycle progression of CML cell lines. A critical role for EZH2 is supported by genetic studies in a mouse CML model. Inactivation of *Ezh2* in conventional conditional mice and through CRISPR/Cas9-mediated gene editing prevents initiation and maintenance of disease and survival of LICs, irrespective of BCR–ABL1 mutational status, and extends survival. Expression of the EZH2 homolog EZH1 is reduced in EZH2-deficient CML LICs, creating a scenario resembling complete loss of PRC2. EZH2 dependence of CML LICs raises prospects for improved therapy of TKI-resistant CML and/or eradication of disease by addition of EZH2 inhibitors.

SIGNIFICANCE: This work defines EZH2 as a selective vulnerability for CML cells and their LICs, regardless of BCR–ABL1 mutational status. Our findings provide an experimental rationale for improving disease eradication through judicious use of EZH2 inhibitors within the context of standard-of-care TKI therapy. *Cancer Discov; 6(11); 1237–47. ©2016 AACR.*

See related article by Scott et al., p. 1248.

INTRODUCTION

Chronic myelogenous leukemia (CML) is a stem cell–driven malignancy induced by the Philadelphia chromosome that generates the fusion oncoprotein BCR–ABL1 (1, 2), which harbors constitutive tyrosine kinase activity. Tyrosine kinase inhibitor (TKI) drugs are highly effective, especially in chronic phase, the early stage of the disease. Nevertheless, disease eradication is challenged by the relative resistance of leukemia-initiating cells (LIC) to cell killing and the emergence of

[1]Division of Hematology/Oncology, Boston Children's Hospital and Department of Pediatric Oncology, Dana-Farber Cancer Institute, Harvard Stem Cell Institute, Harvard Medical School, Boston, Massachusetts. [2]Department of Biostatistics and Computational Biology, Dana-Farber Cancer Institute, Harvard School of Public Heath, Boston, Massachusetts. [3]Department of Medical Oncology, Dana-Farber Cancer Institute, Harvard Medical School, Boston, Massachusetts. [4]Division of Hematology/Oncology, Department of Medicine, University of Massachusetts Medical School, Worcester, Massachusetts. [5]Department of Experimental and Clinical Biomedical Sciences "Mario Serio," University of Florence, Florence, Italy. [6]Department of Medicine, Harvard Medical School, Boston, Massachusetts. [7]Howard Hughes Medical Institute, Boston, Massachusetts.

Note: Supplementary data for this article are available at Cancer Discovery Online (http://cancerdiscovery.aacrjournals.org/).

Current address for J.E. Bradner: Novartis Institute for BioMedical Research, Cambridge, Massachusetts.

Corresponding Author: Stuart H. Orkin, Dana-Farber Cancer Institute, 450 Brookline Avenue, Boston, MA 02215. Phone: 617-919-2042; Fax: 617-632-4367; E-mail: Stuart_Orkin@dfci.harvard.edu

doi: 10.1158/2159-8290.CD-15-1439

TKI-resistant BCR–ABL1 mutants (3–6). Successive generations of TKIs have been developed to overcome intrinsic drug resistance. Treatment with the third-generation TKI ponatinib is effective against CML with the "gatekeeper" T315I mutant BCR–ABL1, but can be accompanied by severe side effects (4, 7). Moreover, ponatinib-resistant CML cells may arise in the setting of recently described compound mutations in BCR–ABL1 (8). To address the limitations of TKIs in CML therapy, alternative pathways required for LICs have been sought. Various targets have been proposed, including heat shock proteins, ALOX5, Wnt/β-catenin, and the hedgehog pathway among others (5). To date, no clinical trials have validated these candidates.

Epigenetic pathways are frequently deregulated in cancer cells. Polycomb Repressive Complex 2 (PRC2) components are often overexpressed and/or somatically mutated in various solid tumors (9–12) and hematopoietic neoplasms (13–17), where cells appear addicted to Polycomb repression. Genetic studies have revealed selective vulnerability of rhabdoid tumors and MLL-AF9 leukemia to Polycomb loss (18, 19). Pharmacologic inhibition of EZH2, the enzymatic subunit of PRC2, efficiently kills some cancer cells, and several clinical trials for EZH2 inhibitors have been initiated (clinicaltrials.gov). Here, we report that CML cells, and notably LICs that are thought to sustain disease, are dependent on EZH2. Because hematopoietic stem cells (HSC) are maintained in the absence of EZH2 (20), this selective vulnerability raises the possibility of leveraging EZH2 as a therapeutic target for eradication of CML.

RESULTS

EZH2 Is Overexpressed in CML LICs, and Its Inactivation Inhibits Cell Growth of Human CML Cell Lines

In a search for potential therapeutic targets essential for CML LICs, we compared gene expression profiles of human CML LICs with normal HSCs ($Lin^-CD34^+CD38^-CD45RA^-CD90^+$; ref. 21). EZH2 was upregulated in LICs at all three phases of disease (Supplementary Fig. S1A). Meanwhile, EZH2 target genes were enriched in LICs compared with HSCs in gene set enrichment analysis (GSEA; ref. 22), suggesting enhanced EZH2 activities in LICs (Supplementary Fig. S1B). Moreover, expression of EZH2, but not other PRC2 components such as EED, appeared dependent on BCR–ABL1 signaling in CML cells, as administration of TKIs (imatinib or dasatinib) reduced EZH2 protein (Supplementary Fig. S1C). Collectively, these findings led us to hypothesize that CML cells, and perhaps their respective LICs, might require, or display "addiction" to, PRC2.

To interrogate the hypothesis, we first tested the response of human CML cells to shRNAs directed to *EZH2*. Two hairpins directed to *EZH2*, which reduced EZH2 protein levels by approximately 70% to 90% (Supplementary Fig. S1D), inhibited the growth of K562 cells (Supplementary Fig. S1E), a consequence of apoptosis and disruption of normal cell cycle (Supplementary Fig. S1F and S1G). Although current TKIs are effective in managing CML in chronic phase, some BCR–ABL1 mutants, such as the "gatekeeper" T315I mutant, present a therapeutic challenge (23). Of note, *BCR–ABL1* mutational status does not change the dependence of CML cells on EZH2, as shRNA knockdown also inhibited growth of K562 cells engineered to express T315I mutant BCR–ABL1 (K562-T315I; Supplementary Fig. S1E).

Genetic Inactivation of *Ezh2* in a Mouse CML Model Blocks Leukemia Development, Independent of Mutational Status of BCR–ABL1

To address the extent of EZH2 dependence for CML *in vivo*, we turned to genetic manipulation of *Ezh2* in mice. We inactivated *Ezh2* in an engineered mouse model of CML. Bone marrow (BM) cells from 5-fluorouracil–treated $Ezh2^{fl/fl}$;Rosa-$EYFP^{fl/fl}$, or Rosa-$EYFP^{fl/fl}$ mice, serving as controls, were transduced with BCR–ABL1-IRES-Cre retrovirus and transplanted into recipients (Fig. 1A). Deletion of *Ezh2*, as monitored by EYFP reporter expression in *Ezh2* knockout (KO) CML mice, markedly delayed disease development, as revealed by reduced leukemic cells ($EYFP^+Mac1^+$) in peripheral blood at days 8 and 12 following transplantation, as compared with the controls and assessed by flow cytometry (Supplementary Fig. S2A and S2B). The total white blood cell count (WBC) was also reduced in *Ezh2* KO CML mice as compared with control CML mice (Supplementary Fig. S2C). Lung hemorrhage and splenomegaly, features of advanced disease in this model, were observed in control CML mice 2 weeks after bone marrow transplantation (BMT), but not observed in *Ezh2* KO CML mice (Supplementary Fig. S2D). *Ezh2* deletion prolonged survival, though mice eventually succumbed to CML due to outgrowth of rare cells with incomplete excision of *Ezh2* alleles (Supplementary Fig. S2E and data not shown).

Figure 1. *Ezh2* inactivation inhibits initiation/progression of CML and establishment of secondary leukemia from existing LICs. **A,** protocol for induction of *Ezh2* deleted (*Ezh2* KO) or control (Con) CML in mice. **B,** FACS plots showing percentages of leukemic cells in peripheral blood of control and *Ezh2* KO-T315I CML mice at indicated days after BMT. **C,** percentage of T315I CML cells, as shown in **B**. $n = 10$ for both control and *Ezh2* KO CML mice. $P = 0.21$ for day 6, and $P < 0.0001$ for days 9, 12, and 14, as determined by the Student *t* test. **D,** peripheral WBC of control ($n = 5$) and *Ezh2* KO CML mice ($n = 5$), determined at day 14 after BMT. $P < 0.0001$ as determined by the Student *t* test. **E,** survival curve of control ($n = 10$) and *Ezh2* KO CML mice ($n = 10$). $P < 0.0001$, as determined by Gehan–Breslow–Wilcoxon test. **F,** percentage (left) and cell number (right) of LICs ($EYFP^+Lin^-c\text{-}Kit^+Sca1^+$) in control ($n = 9$) and *Ezh2* KO ($n = 21$) CML mice, measuring at day 14 after BMT. $P = 0.001$ for the percentage and $P = 0.003$ for the cell number of LICs, as determined by the Student *t* test. **G,** experimental protocol for assessing impact of *Ezh2* loss in LICs for leukemia development in secondary recipients. **H,** FACS plots showing percentages of Cre^+ (GFP^+EYFP^+) and Cre^- (GFP^+EYFP^-) secondary leukemic cells in peripheral blood of control and *Ezh2* KO CML mice at days 7, 11, and 14 after BMT. Samples analyzed right before second BMT were designated as day 0. **I,** ratio of Cre^+ (GFP^+EYFP^+) versus Cre^- (GFP^+EYFP^-) secondary leukemic cells, as shown in **H,** at the indicated days after second BMT in control or *Ezh2* KO 2nd CML mice. Only one sample each for day 0 was analyzed and thus was excluded from statistical analysis. $P < 0.0001$ for days 7, 11, and 14 and $P = 0.04$ for day 17, as determined by the Student *t* test. **J,** survival curve of control ($n = 6$) and *Ezh2* KO ($n = 5$) secondary CML mice. $P = 0.036$, as determined by Gehan–Breslow–Wilcoxon test. Results shown in **B–J** are representative of at least two repeat experiments.

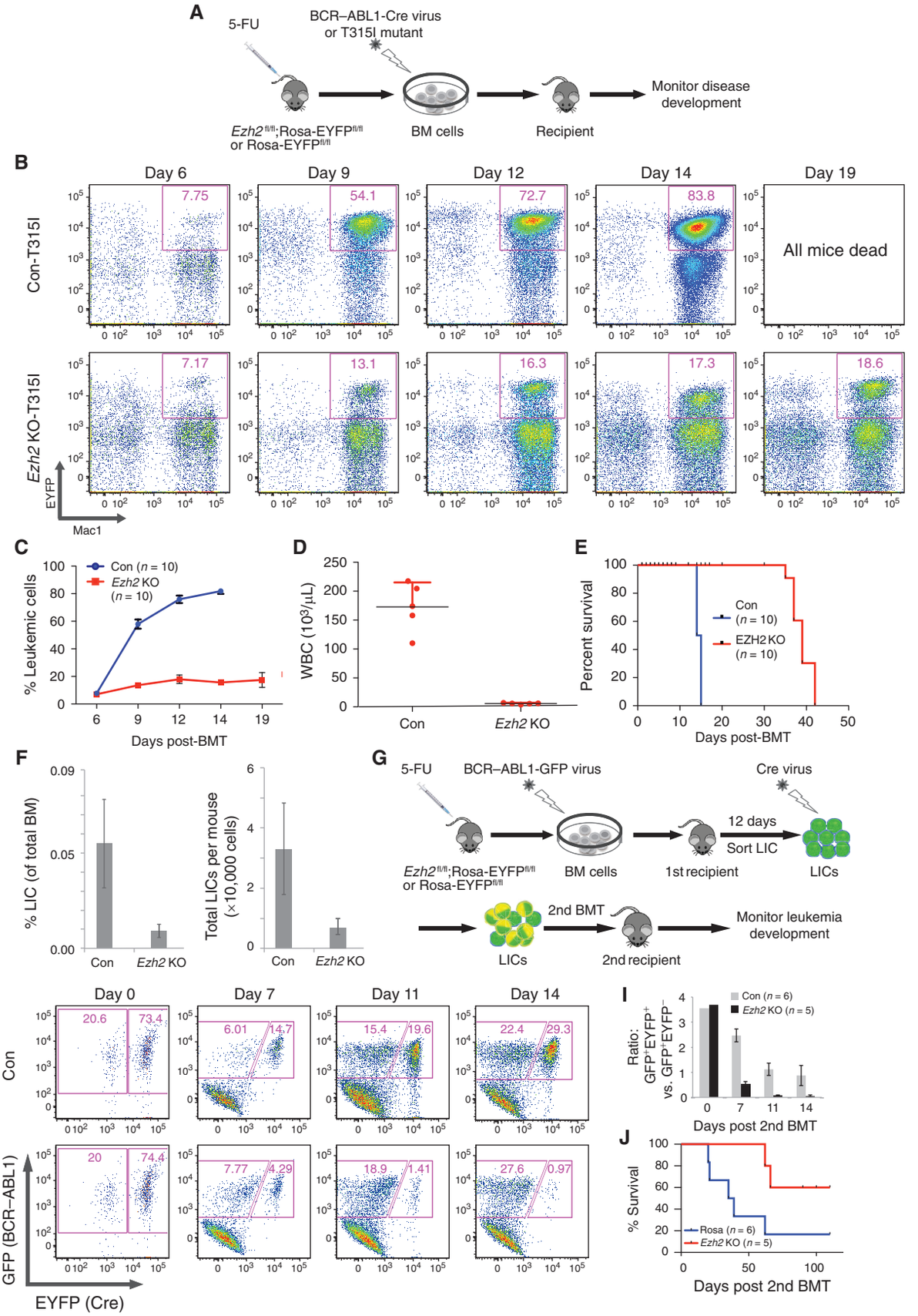

Together, these data demonstrate that leukemia initiation and development are dependent on EZH2.

To assess whether EZH2 is also required for T315I mutant CML, we induced CML with T315I mutant BCR–ABL1 (Fig. 1A). CML progressed rapidly in control T315I CML mice and culminated with heavy leukemia load and death of animals at approximately 2 weeks after BMT. In contrast, leukemia development was markedly blunted in *Ezh2* KO CML mice, and survival was greatly extended (Fig. 1B–E). Thus, the requirement for EZH2 in CML appears independent of the mutational status of BCR–ABL1.

EZH2 Is Required for Maintenance and Function of CML LICs

CML is a stem-cell disorder in which disease initiation and maintenance rely on LICs, a population of cells enriched in the $Lin^-c\text{-}Kit^+Sca1^+$ population in CML mice (24, 25). To assess the impact of EZH2 loss on CML LICs, we first determined the frequency and total cell number of LICs in control or EZH2 KO CML mice. Loss of EZH2 greatly reduced LIC frequency, as well as cell number, in *Ezh2* KO CML mice, compared with control CML mice, indicating sensitivity of LICs to EZH2 loss (Fig. 1F). In the experimental setting depicted in Fig. 1A where Cre-expressing virus is transduced into normal hematopoietic stem/progenitor cells (HSPC) to inactivate EZH2, it is not possible to distinguish between requirements of LICs for EZH2 and requirements for EZH2 in transforming HSCs into LICs by BCR–ABL1.

To interrogate more directly the requirement of LICs for EZH2, we determined the consequences of inactivating *Ezh2* in preexisting LICs. To this end, control or $Ezh2^{fl/fl}$ LICs from primary CML mice, induced by BCR–ABL1-IRES-GFP virus, were isolated by fluorescence-activated cell sorting (FACS), transduced with Cre virus, and then transplanted into secondary recipients (Fig. 1G). Control CML LICs, with (GFP^+EYFP^+) or without (GFP^+EYFP^-) Cre virus transduction, contributed comparably to the development of secondary leukemia (Fig. 1H and I). In contrast, uninfected $Ezh2^{fl/fl}$ LICs (GFP^+EYFP^-) greatly outcompeted *Ezh2* KO LICs (GFP^+EYFP^+) in the secondary leukemia, and the percentage of *Ezh2* KO LIC–derived secondary leukemic cells decreased over time (Fig. 1H and I). Accordingly, deletion of *Ezh2* in CML LICs prolonged survival of secondary CML mice (Fig. 1J). Notably, of the 2 *Ezh2* KO secondary CML mice that died in this study, 1 died of GFP^+EYFP^- (Cre negative) CML and the second was euthanized for conditions unrelated to CML. In contrast, biopsy showed that all control secondary CML mice died of CML. Taken together, these results indicate that CML LICs require EZH2 for their maintenance and ability to initiate leukemia on transplantation.

Catalytic Activity of EZH2 Is Required for CML Cells

Genetic study in the mouse CML model demonstrated that EZH2 is required for CML and its LICs, and therefore suggests that EZH2, a histone methyltransferase, might be targeted for CML therapy. The findings in Cre conditional mice, in which intact protein is eliminated, fail to exclude a noncatalytic role of EZH2 for CML cells (26). We next determined whether catalytic activity of EZH2 is required for CML cells. Exogenous EZH2, either wild-type or a mutant with three substitutions (F677I, H689A, and R727K) that result in loss of catalytic activity (27, 28), was expressed in K562 cells. Endogenous *EZH2* was then deleted by CRISPR/Cas9-mediated gene editing (Fig. 2A). Exogenous wild-type EZH2 rescued growth and survival of cells with homozygous loss of endogenous EZH2. In contrast, exogenous mutant EZH2 expression failed to rescue cells lacking a functional endogenous *EZH2* allele (Fig. 2B). These data provide strong genetic evidence that the catalytic activity of EZH2 is required for viability of CML cells.

We next tested several small-molecule catalytic inhibitors of EZH2: GSK126 (29), UNC1999 (30, 31), and JQEZ5 (32) as well as an inactive analogue of JQEZ5, JQEZ23 (Supplementary Fig. S3A). The inhibitors, but not the inactive analogue, effectively reduced the global level of the PRC2-associated mark, H3K27me3, in K562 cells (Supplementary Fig. S3B) and suppressed cell growth in a dose-dependent manner in K562 and KBM5 CML cells, as well as corresponding T315I derivative lines (Fig. 2C and Supplementary Fig. S3C and S3D). These results provide further evidence that human CML cells rely on EZH2, and more specifically its enzymatic activity, to support cell survival and growth, independent of the mutational status of BCR–ABL1.

To assess EZH2 dependence of primary human CML stem/progenitor cells, we performed colony formation assays in the presence of EZH2 inhibitors. JQEZ5 and UNC1999 inhibited colony formation of primary human $CD34^+$ CML stem/progenitor cells (Fig. 2D and E and Supplementary Fig. S3E and S3F). JQEZ5 did not appreciably affect colony formation of normal human $CD34^+$ HSPCs, although at higher concentrations, UNC1999 modestly inhibited their colony formation (Fig. 2D and E and Supplementary Fig. S3E and S3F). This is likely due to moderate inhibition of EZH1 by UNC1999 (30). The inhibitors also reduced colony formation of primary CML cells with the T315I mutation (Fig. 2E and Supplementary Fig. S3F). Together, these results demonstrate that colony formation of human CML stem/progenitor cells is sensitive to EZH2 inhibition. This conclusion is compatible with our observations presented below regarding the dependence of mouse CML LICs, but not HSCs (20), on EZH2.

EZH2 Inactivation in CML LICs Creates a Context Resembling Total Loss of PRC2

To probe potential molecular mechanisms for the dependence of CML LICs on EZH2, gene expression profiles of *EZH2* KO and *EZH2* wild-type CML LICs, together with *EZH2* KO, *EED* KO, and wild-type HSCs, were compared. *EZH1* mRNA expression decreased in LICs, in comparison with HSCs, both in mouse and in human (Fig. 3A and Supplementary Fig. S4A). Of note, the level of *EZH1* was further reduced in CML LICs lacking *EZH2* (Fig. 3A). A striking similarity in gene expression changes was observed on comparison of *EZH2* KO LICs and *EED* KO HSCs. For example, gene expression changes between *EZH2* loss in LICs and *EED* deletion in HSCs were more similar than between *EZH2* deletion and *EED* deletion in HSCs (Fig. 3B). In addition, we found that a subset of genes upregulated in *EZH2* KO LICs as compared with control LICs was more enriched in *EED* KO HSCs than in *EZH2* KO HSCs in comparison with wild-type HSCs, as revealed by GSEA analysis (Fig. 3C). *EZH2* KO in CML LICs

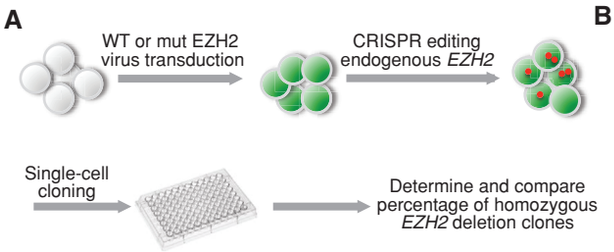

B

	WT exogenous EZH2	Mut exogenous EZH2
No deletion	78 (64.4%)	68 (69.4%)
One allele deleted	33 (27.3%)	30 (30.6%)
Both alleles deleted	10 (8.26%)	0

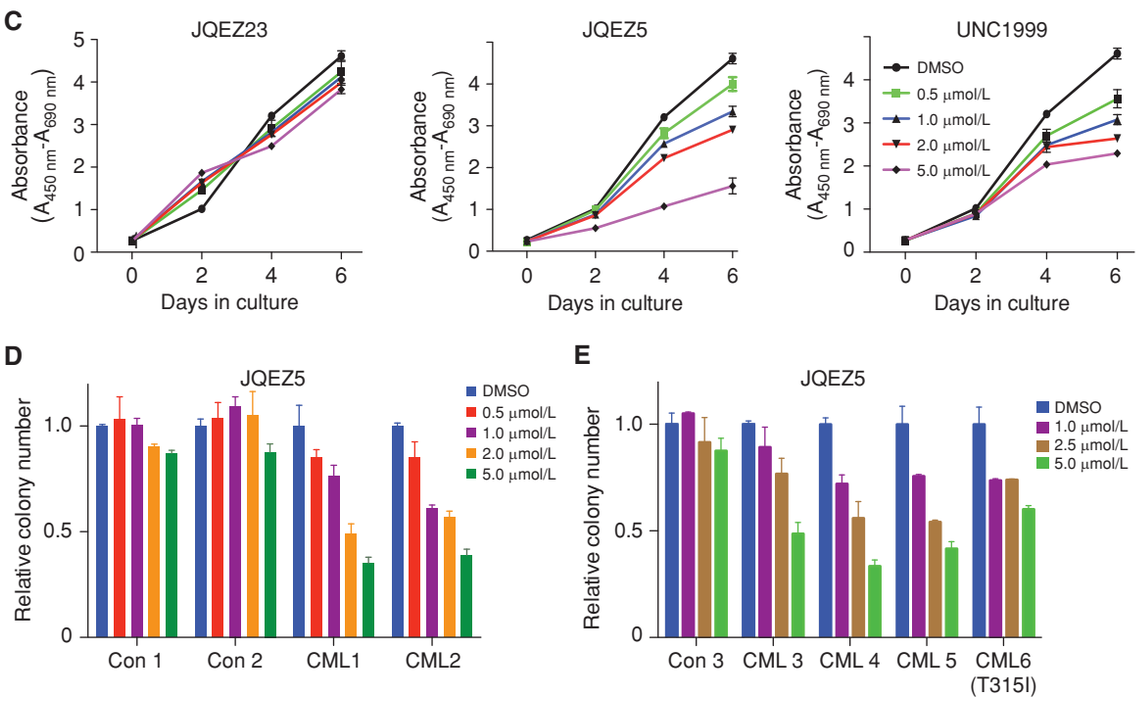

Figure 2. EZH2 catalytic activity is required for CML cells and their stem/progenitor cells. **A,** experimental protocol for rescue of CML cells with either wild-type (WT) or catalytically inactive EZH2. The endogenous *EZH2* was inactivated by CRISPR/Cas9-mediated gene editing. **B,** table presenting numbers and percentage of single-cell clones with 0, 1, or 2 alleles of endogenous *EZH2* deleted. **C,** growth curve of K562 cells treated with EZH2 catalytic activity inhibitors UNC1999 and JQEZ5 or an inactive analogue, JQEZ23. Cells were cultured with compounds at the indicated concentrations for 6 days, and cell proliferation was determined by WST-1 cell proliferation assay every other day. Absorbance (A_{450}–A_{690}) of DMSO-treated samples was set as 1, and the ratios of absorbance in EZH2 inhibitors–treated samples relative to DMSO-treated samples were plotted. Data shown as mean ± SD. Three biological replicates were performed for each sample, and two repeat experiments were performed. **D** and **E,** relative colony numbers of human BM $CD34^+$ CML stem/progenitor cells (**D**) or total primary CML BM cells (**E**), along with their respective normal cells (Con) plated in media with DMSO or with different concentrations of JQEZ5. Colonies were enumerated at day 9 after plating. The number of colonies in the DMSO-treated group was set as 1, and ratios of colonies of the JQEZ5-treated group relative to DMSO-treated group were plotted. Each sample was plated in duplicate, and two repeat experiments were performed. Data shown as mean ± SD. *P* values for JQEZ3 and DMSO comparison are 0.30, 0.34, 0.23, and 0.21 for a concentration of 0.5, 1, 2, and 5 μmol/L respectively; for JQEZ5 and DMSO comparison the *P* values are 0.002, 0.003, 0.002, and 0.001 for a concentration of 0.5, 1, 2, and 5 μmol/L, respectively; for UNC1999 and DMSO comparison, these values are 0.003, 0.003, 0.006, and 0.004 for a concentration of 0.5, 1, 2, and 5 μmol/L, respectively.

induced changes in the expression of many genes belonging to different functional groups, or gene sets. A substantial portion (143 of a total of 353) of these gene sets, enriched in *EZH2* KO LICs as compared with control LICs, were also enriched in *EED* KO HSCs as compared with wild-type HSCs, but not in *EZH2* KO HSCs as compared with their wild-type counterparts (Fig. 3D and Supplementary Table S1). Taken together, these findings indicate that the impact of EZH2 loss in LICs resembles, in part, EED loss in HSCs. EZH2, or its close homolog EZH1, together with EED and SUZ12 comprise the core subunits of PRC2 complexes. Inactivation of EED disrupts the integrity of the PRC2 complexes and completely disables their functions. These data strongly suggest that inactivation of EZH2 in LICs creates a situation mimicking complete loss of PRC2.

Enhanced repression of PRC2 target genes is a common feature of many cancers with overexpressed PRC2 components. EZH2 overexpression in CML LICs, compared with normal HSCs, was associated with downregulation of 263 genes (at 2-fold cutoff). Twenty-seven of these 263 genes were

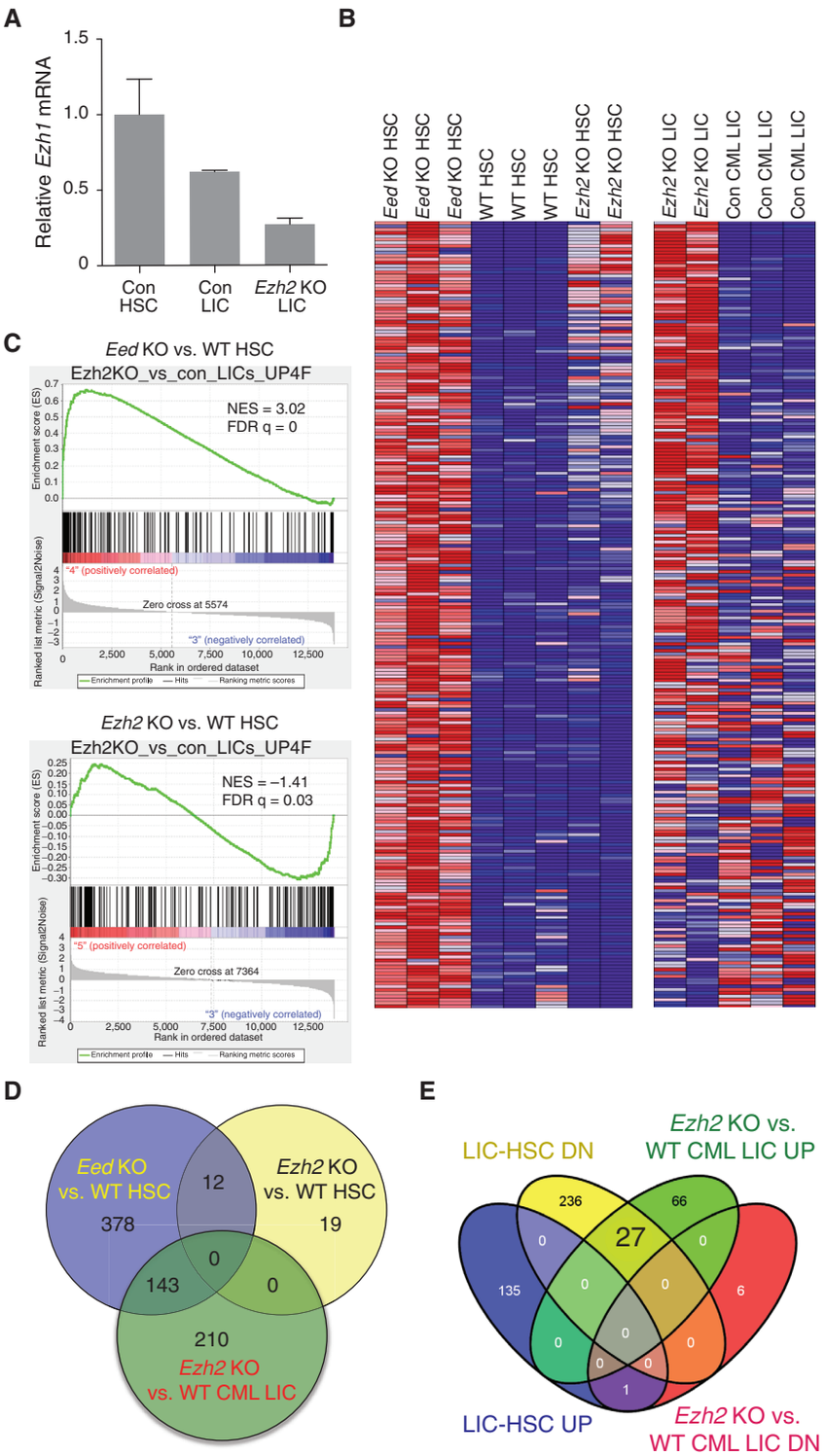

Figure 3. EZH2 inactivation in CML LICs creates a context mimicking complete loss of PRC2. **A,** relative abundances of *Ezh1* mRNA transcripts in normal LKS cells (Lin$^-$ c-Kit$^+$Sca1$^+$) (Con HSC), *Ezh2* wild-type (WT) primary CML (CML LIC), and *Ezh2* KO primary CML LICs (*Ezh2* KO LIC), determined at day 14 after BMT. Value of *Ezh1* mRNA transcripts in normal LKS cells was set to 1, and ratios of *Ezh1* mRNA transcripts in control CML LICs or *Ezh2* KO LICs relative to normal LKS cells were plotted. Data shown as mean ± SD. $P = 0.038$ for wild-type LKS cells vs. control CML LICs and $P = 0.002$ for control CML vs. *Ezh2* KO CML LICs. **B,** heat maps comparing expression of genes, upregulated in *Eed* KO vs. wild-type HSCs (4-fold cutoff, 239 probes for 193 genes), among *Eed* KO, *Ezh2* KO, and WT HSCs, as well as between *Ezh2* KO vs. control CML LICs. **C,** genes upregulated in *Ezh2* KO vs. control CML LICs (4-fold cutoff) are enriched in *Eed* KO (left) but not in *Ezh2* KO HSCs (right), in comparison with wild-type HSCs, as assessed by GSEA. **D,** Venn diagram showing overlap of gene sets enriched in different comparisons. Affymetrix array expression values of *Eed* KO vs. WT HSCs, *Ezh2* KO vs. WT HSCs, and *Ezh2* KO vs. control CML LICs were analyzed in GSEA for the enrichment of gene sets in C2 (curated gene sets), C4 (computational gene sets), C6 (oncogenic signatures), and C7 (immunologic signatures) from Molecular Signature Dataset (MSigDB). Gene sets enriched in KO cells, for each comparison group, were filtered for FDR q < 0.01, and the results plotted in this Venn diagram. **E,** Venn diagram depicting the correlation of the following 4 gene sets: (1) upregulated (UP) genes in control CML LICs vs. normal HSCs (LKS cells), depicted as the blue oval; (2) downregulated (DN) genes in control CML LICs vs. normal HSCs, depicted as the yellow oval; (3) upregulated genes in *Ezh2* KO LICs vs. control CML LICs, depicted as the green oval; (4) downregulated genes in *Ezh2* KO LICs vs. control CML LICs, depicted as the red oval. A fold-change cutoff of ±2.0 and FDR < 0.05 was applied to all comparison groups.

upregulated in *EZH2* KO CML LICs, comprising about 1/3 of the total upregulated genes in *EZH2* KO LICs compared with control LICs (at 2-fold cutoff; Fig. 4E and Supplementary Table S2). Among these 27 "derepressed" genes, *Trp53inp1, Phlpp1, H19,* and *Cdkn2c* are associated with apoptosis or inhibition of cell proliferation (33–36). Accordingly, we observed enrichment of gene sets including p53 targets, p53 pathways, and MDM4 targets in *EZH2* KO LICs compared with control LICs, as revealed by GSEA analysis. Conversely, gene sets that favor cell growth were enriched in control CML LICs (Supplementary Fig. S4B and data not shown). Collectively, these data suggest that PRC2 suppresses apoptosis

and proliferation inhibitor genes in CML LICs to support cell survival and growth. Consequently, inactivation of EZH2 is associated with increased expression of these genes, and subsequent growth inhibition and cell death.

EZH2 Inactivation in Existing Disease Induces Disease Regression

To be considered further as a target for CML treatment, manipulation of EZH2 in existing disease should lead to clearance or regression of disease. We explored this possibility by inactivating *Ezh2* through CRISPR/Cas9-mediated gene editing in mice with preexisting CML. To achieve temporal and highly efficient gene inactivation, we employed a doxycycline-inducible Cas9-expressing mouse line developed in our lab (to be described elsewhere). For efficient editing and inactivation of EZH2 catalytic function in the *in vivo* setting, we chose an *Ezh2* guide RNA (gRNA) that targets the SET domain (37). This gRNA achieves greater than 85% allele editing after Cas9 induction in a B-cell line transformed from the doxycycline-inducible Cas9 strain (Supplementary Fig. S5A). CRISPR/Cas9-mediated gene editing of the *Ezh2* locus significantly reduced global 3mH3K27, although seemingly without an appreciable change in total EZH2 protein (Supplementary Fig. S5B). This is likely due to inability of this SDS-PAGE Western blot analysis to resolve wild-type full-length EZH2 (746aa) from mutant EZH2 proteins caused by indels that are just 50 to 60aa shorter.

To test the role of EZH2 in established disease, we generated primary CML in mice with BCR–ABL1-GFP virus plus *Ezh2* gRNA virus or an empty virus. CML stem/progenitor cells were then transplanted into recipients to generate mice with secondary leukemia. Upon establishment of secondary leukemia, recipients were treated with doxycycline to induce Cas9 expression and observed over time (Fig. 4A). *Ezh2*–CRISPR/Cas9-mediated gene editing in mice with established CML slowed disease progression, as compared with the empty virus–transduced cohort also treated with doxycycline. Of special note, disease regression subsequently occurred in all CML mice expressing *Ezh2* gRNA (Fig. 4B–D and Supplementary Fig. S5C). Consequently, CRISPR/Cas9-mediated *Ezh2* inactivation in CML mice greatly extended survival, as compared with the empty virus cohort (Fig. 4E).

Leukemic cells were sorted at different times, and the frequency of indels was determined by Tracking of Indels by DEcomposition (TIDE) analysis (ref. 38; Supplementary Fig. S5C). The overall dynamics of indels at the population level are likely complex, as cells with inactivation of both *EZH2* alleles are presumably eliminated, whereas those with one or two active alleles remain and may sustain editing events in the presence of continued Cas9 expression. Accordingly, indel frequency of leukemic cells is predicted to rise to approximately 50% and plateau, at which point all leukemic cells have one edited allele and the other is inactivated in those cells destined for elimination.

DISCUSSION

TKI therapy has transformed CML management, turning a lethal disorder into a chronic condition. However, challenges remain in conventional TKI therapy for CML, including the relative resistance of CML LICs to TKIs and the appearance of TKI-resistant BCR–ABL1 mutants. Candidate targets of alternative pathways have been explored, but none have been validated in clinical trials. Recently, a PPARγ agonist was reported to sensitize LICs to TKIs, likely by coaxing LICs into cycle, and thereby raised the possibility of combination therapy for disease eradication (39). Simultaneous targeting of p53 and c-MYC has recently been reported as another strategy (40).

Here, we have identified and validated EZH2 as a selective vulnerability for CML LICs. Inactivation of *Ezh2* in the engineered mouse model of CML blocks leukemia initiation/development and impairs CML LICs. More importantly, CRISPR/Cas9 domain–directed editing to inactivate *Ezh2* in mice with existing disease leads to disease regression and a marked improvement in survival. The latter also suggests that EZH2 catalytic activity is required for CML cells *in vivo*, which is further supported by the rescue experiment where wild-type EZH2, but not a catalytically inactive mutant, rescues CML cells with homozygous loss of endogenous EZH2. In addition to providing additional *in vivo* genetic evidence in support of a critical role for EZH2 in CML maintenance, our dox-inducible CRISPR/Cas9 gene-editing experimental system should have broad applicability in other cancer models.

EZH2 inactivation in human CML cells leads to cell growth inhibition and inhibition of colony formation by primary CML stem/progenitor cells. Of note, dependence on EZH2 is independent of the mutational status of BCR–ABL1. EZH1 expression is reduced in CML LICs upon *EZH2* inactivation, which may lead to impairment of PRC2 function and failure of LIC maintenance or survival. The consequence of EZH2 loss in the context of normal HSCs differs, in that EZH1 expression is maintained at a higher level. Although the mechanistic basis for this difference is unclear, the presence of EZH1 in HSCs partially compensates for EZH2 loss, preserves PRC2 function, and protects cells from the deleterious effects of complete PRC2 loss. The dependence of CML LICs on EZH2 appears quite selective in comparison with several other proposed targets for enhanced CML therapy (5), the majority of which are required for normal hematopoiesis and/or maintenance of HSCs. Such selectivity predicts existence of a therapeutic window for the administration of EZH2 inhibitors to eliminate CML LICs without adversely affecting overall hematopoiesis. Nevertheless, *EZH2* inactivation may also be tumorigenic (14, 17, 41) in some circumstances. Although transient pharmacologic inhibition of EZH2 is unlikely to mimic genetic loss of EZH2, caution would need to be taken to monitor any undesired effects of EZH2 inhibitors in therapy.

In conclusion, we have genetically defined a dependence of CML LICs on EZH2, thereby establishing a potential target for improved therapy. Given the current clinical development of EZH2 inhibitors, our findings provide an experimental rationale for incorporating these agents into therapy of CML directed at disease eradication. We propose that inhibition of EZH2 should be considered as an additional strategy to circumvent intrinsic resistance to TKIs and eliminate CML LICs.

In an accompanying article in this issue, Scott and colleagues independently identify the dependence of CML on EZH2 (42).

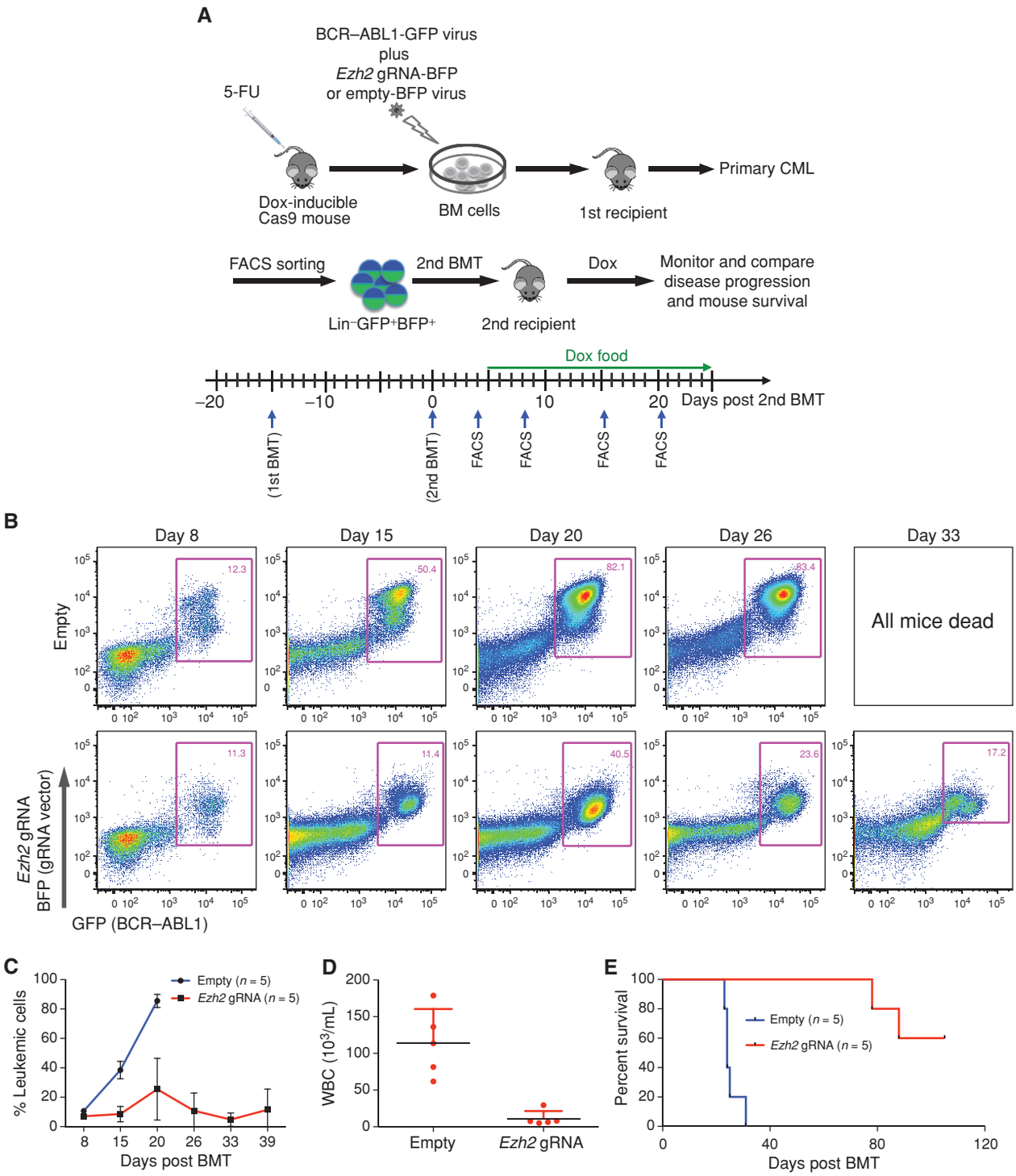

Figure 4. CRISPR/Cas9-mediated *Ezh2* inactivation in existing CML induces disease regression and extends survival. **A,** protocol for generation of *Ezh2* gRNA and empty-vector control CML followed by doxycycline-induced Cas9 expression and *Ezh2* inactivation. **B,** FACS plots showing percentages of leukemic cells within Mac1$^+$ population in peripheral blood of *Ezh2* gRNA or empty-vector control CML mice at different times after BMT. **C,** percentage of CML cells in peripheral blood of *Ezh2* gRNA or empty-vector control CML mice. $n = 5$ for both *Ezh2* gRNA and empty-vector control CML mice. $P = 0.06$ for day 6, and $P < 0.001$ for days 15 and 20 as determined by the Student *t* test. Only one Empty CML mouse survived at day 26 and was excluded for statistical analysis. **D,** peripheral WBC of *Ezh2* gRNA ($n = 5$) and Empty CML mice ($n = 5$), determined at day 20 after BMT. $P = 0.001$ as determined by the Student *t* test. **E,** survival curve of *Ezh2* gRNA ($n = 5$) and Empty CML mice ($n = 5$). Of note, CML is unlikely to be the primary cause of death for the 2 mice in the *Ezh2* gRNA group that succumbed, as CML cells were only 34.2% and 0.2% of total white blood cells respectively at the time of death. $P = 0.003$, as determined by Gehan–Breslow–Wilcoxon test.

METHODS

Experimental Animals

C57BL/6 and Rosa26-EYFP$^{fl/fl}$ (43) lines were obtained from The Jackson Laboratory. 129/B6 mice were purchased from Taconic. The doxycycline-inducible Cas9-expressing line was created in the Orkin laboratory and will be described elsewhere. *Ezh2* conditional KO mice have been described (44) and were maintained on a C57BL/6 background. Animals were maintained in the animal facility at Boston Children's Hospital. The Institutional Animal Ethics Committee approved all animal experiments.

Cell Lines

KBM5 and KBM5-T315I cells were generously provided by Dr. Ralph B. Arlinghaus (The University of Texas MD Anderson Cancer Center) in 2013 without further authentication. K562 cells were obtained from the ATCC (CCL-243; ATCC) in 2012 without further authentication. The T315I BCR–ABL1 derivative line was generated by expansion of FACS-sorted GFP$^+$ cells from BCR–ABL1(T315I)-IRES-GFP retrovirus–transduced K562 cells. All cells were cultured in Iscove's Modified Dulbecco's Medium (IMDM) media supplemented with 10% FBS, 50 μmol/L 2-mercaptoethanol, and 100 U/mL penicillin/streptomycin. Cells were tested by PCR-based assay to verify that they were free of *Mycoplasma* contamination.

Rescue of CRISPR Inactivated Endogenous EZH2 with Exogenous EZH2 Enforced Expression

K562 cells were infected with lentivirus expressing a GFP marker gene plus either wild-type EZH2 or a mutant with three substitutions (F677I, H689A, and R727K) that render the catalytic domain inactive. Codons of both wild-type and mutant EZH2 had been modified so that *EZH2* gRNA will recognize endogenous *EZH2*, but not the exogenous *EZH2*. *EZH2* gRNAs were cloned into CRISPR Nuclease Vector-OFP purchased from ThermoFisher. GFP/OFP double-positive cells were FACS-sorted 24 hours after transfection for single-cell cloning. Genomic DNA was extracted from individual clone and PCR performed for genotyping. Sequences of gRNA sequences are GAGCT CATTGCGCGGGACTA and TGCGACTGAGACAGCTCAAG.

Bone Marrow Transduction and Transplantation

BM transduction and transplantation procedures have been described (45). Eight-to-10-week-old donor mice were primed by intravenous injection of 5-fluorouracil (200 mg/kg; Sigma) 5 days before harvest. BM cells were plated at 2×10^7 cells per 10-cm plate in prestimulation medium (DMEM, 15% FBS, 100 ng/mL recombinant murine SCF, 10 ng/mL recombinant murine IL3, 10 ng/mL recombinant murine IL6, 50 μmol/L 2-mercaptoethanol, and 100 U/mL penicillin/streptomycin). Cytokines were purchased from R&D systems. Cells were incubated overnight at 37°C. Virus transduction was performed by suspending cells in prestimulation media containing 50% virus supernatant and supplemented with 10 μg/mL polybrene (Millipore). Cells were then spun for 60 minutes at 700 *g* and incubated at 37°C for 2 to 4 hours before transfer to fresh media, and then incubated at 37°C overnight. A second round of transduction was performed, and the cells were collected 3 hours later, washed once in Hank's Balanced Salt Solution (HBSS), and counted. Cells (0.5×10^6) in 0.4 mL HBSS were injected via tail vein to the recipient mice (congenic, 8–10 weeks old), which had received two doses of 400-cGy gamma irradiation separated by at least 3 hours. All recipient mice were mixed after secondary irradiation and randomly separated into two groups, one of which received BCR–ABL1-IRES-Cre virus–transduced Rosa-EYFP$^{fl/fl}$ BM cells, and the other of which received the same virus-transduced *Ezh2*$^{fl/fl}$;Rosa-EYFP$^{fl/fl}$ BM cells.

Retrovirus Transduction of LICs and Secondary Transplants

To assess dependence of LICs on EZH2, primary LICs (GFP$^+$Lin$^-$c-Kit$^+$Sca1$^+$) were purified by FACS sorting from CML induced by BCR–ABL1-IRES-GFP virus–transduced *Ezh2*$^{fl/fl}$;Rosa-EYFP$^{fl/fl}$ or Rosa-EYFP$^{fl/fl}$ BM cells, 12 days after BMT. Primary LICs were transduced with Cre retrovirus for two rounds. Thirty-six hours after second round Cre virus transduction, 0.2×10^6 cells were transplanted into second recipients, which had received two doses of 400-cGy gamma irradiation separated by at least 3 hours, together with 0.5×10^6 C57BL/6 BM cells. Leukemia progression was determined by percentage of leukemic cells in the blood by flow cytometry.

CRISPR Inactivation of Ezh2 in Existing Mouse CML

Ezh2 gRNA targeting the SET domain of *Ezh2* has been previously described (37). Primary CML was derived as described above, using doxycycline-inducible Cas9-expressing mice as BM donors (B6/129 background). Lin$^-$GFP$^+$BFP$^+$ leukemia stem/progenitor cells were FACS sorted from BM and spleen of primary CML. Half a million sorted cells were mixed with 2 million B6/129 BM cells and transplanted into secondary recipients (B6/129). Four days after secondary BMT, peripheral blood was assessed by FACS to confirm the establishment of leukemia, and mice were fed with doxycycline food from day 5 after BMT and thereafter. Mac1$^+$BFP$^+$GFP$^+$ cells were sorted from each secondary CML mouse at different times, genomic DNA extracted, and DNA sequences flanking Cas9 cutting site amplified by PCR, which were sequenced and percentages of edited *Ezh2* alleles were calculated by TIDE analysis.

Lentiviral Vectors and Viral Infection

shRNAs, constructed in pLKO.1-puro lentiviral vector, targeting human EZH2 (RefSeq ID: NM_004456) were obtained from the Mission shRNA collection (Sigma-Aldrich). The sequences of shRNA EZH2 #2 and #3 were: CCGGGCTAGGTTAATTGGGACCAAACTC GAGTTTGGTCCCAATTAACCTAGCTTTTTG and CCGGCCCAAC ATAGATGGACCAAATCTCGAGATTTGGTCCATCTATGTTG-GGTTTTTG, respectively.

Flow Cytometry

For assessing leukemic cells in the blood, erythrocyte-lysed blood samples were suspended in FACS staining buffer (PBS supplemented with 4% FBS) and incubated with Fc-Block (purified CD16/CD32, clone 93) for 10 minutes on ice before addition of APC-Cy7–conjugated B220 (RA3-6B2) and APC-conjugated CD11b (M1/70) antibodies, and incubated on ice for 20 minutes. Cells were then washed and suspended in FACS staining buffer with 0.1 μg/mL of DAPI (Invitrogen).

For analysis or prospective isolation of phenotypic LICs, BM cells were suspended in FACS staining buffer and first incubated with Fc-Block for 10 minutes on ice, and then with biotin-conjugated lineage marker antibodies [CD3e (145-2C11), CD4 (GK1.5), CD5 (53-7.3), CD8a (53-6.7), CD11b (M1/70), B220 (RA3-6B2), Gr1 (RB6-8C5), and Ter119 (TER119)] on ice for 20 minutes. After a wash with FACS staining buffer, cells were incubated with Percp-Cy5.5–conjugated streptavidin, PE-Cy7–conjugated Sca1 (D7), and APC-conjugated c-Kit (2B8) on ice for 20 minutes. Cells were then washed, and suspended in FACS staining buffer with 0.1 μg/mL of DAPI (Invitrogen).

For analysis of apoptosis, cells were washed and suspended in Annexin V staining buffer (10 mmol/L M HEPES, pH 7.4; 140 mmol/L NaCl; 2.5 mmol/L $CaCl_2$) before addition of APC-conjugated Annexin V (BMS306APC/100; eBioscience) and incubation for 30 minutes at room temperature. Cells were then washed and suspended in Annexin V staining buffer supplemented with 0.1 μg/mL DAPI (Invitrogen).

All samples were filtered through 40 μm mesh (BD Bioscience) before running on LSR II/LSR Fortessa (BD Bioscience) for analysis or on FACSAria II SORP (BD Bioscience) for cell sorting. Fluorescence compensation or spillover was calculated automatically using

single color controls and Diva software. FACS data were analyzed with FlowJo software (Tree Star).

BrdUrd Incorporation and Cell-Cycle Analysis

Determination of cell-cycle distribution by flow cytometry detection of BrdUrd pulse-labeled cells was performed with the APC BrdU Flow Kit (BD Bioscience) following the manufacturer's instructions. Briefly, cells were incubated with BrdUrd (final concentration 10 mmol/L) containing media for 60 minutes. After a PBS wash, cells were fixed with paraformaldehyde, permeabilized, and treated with DNase I to expose BrdUrd, incorporated in DNA. After washing, cells were incubated with APC-conjugated BrdUrd antibody for 20 minutes on ice. Stained cells were washed and suspended in FACS staining buffer with 0.1 μg/mL of DAPI for flow cytometry.

Global Gene Expression Profiling

Phenotypic CML LICs ($EYFP^+Lin^-c\text{-}Kit^+Sca1^+$) were purified from *Ezh2* KO or control CML mice, 2 weeks after BMT. Each sample was sorted from BM cells pooled from 4 to 6 CML mice and double-sorted to increase the purity of the designated cell population. During the second sort, target cells were directly deposited into a 1.5 mL DNA LoBind tube (Eppendoff) filled with 350 μL RLT PLUS buffer (Qiagen) supplemented with 2-Mercaptoethanol (Sigma). Total RNA was isolated using the RNeasy Micro Plus Kit (Qiagen), reverse transcribed, amplified with the WT-Ovation Pico RNA Amplification System V2 (NuGen Technologies), labeled (NuGen; Encore Biotin Module), and hybridized to Affymetrix mouse 430A 2.0 arrays. Data were normalized and analyzed with GenePattern and GSEA. Gene expression data have been deposited in the Gene Expression Omnibus (GEO) under accession numbers GSE85744 and GSE51084.

Published data sets (21) deposited on GEO (GSE47927) were used for comparative analysis of gene expression between human CML LICs and normal HSCs.

Western Blot Analysis

Whole-cell lysates were prepared in RIPA buffer and proteins separated on SDS-PAGE gel. Proteins were then detected with anti-H3 (Ab1791; Abcam), anti-H3K27me3 (07-449; Millipore), anti–c-ABL (sc-131; Santa Cruz Biotechnology), anti–β-Actin (Ab8226; Abcam), and anti-GAPDH (#2118S; Cell Signaling Technology) primary antibodies plus proper horseradish peroxidase–conjugated secondary antibodies (Santa Cruz Biotechnology) and ECL reagents.

Human Samples

Primary human CML samples were obtained from the Pasquarello Tissue Bank of Dana-Farber Cancer Institute. Patient samples were collected under Dana-Farber/Harvard Cancer Center Protocol 01-206 with consent of patients and their families. Primary human adult $CD34^+$ BM HSPCs were purchased from Stem Cell Technology.

Colony Formation Assay

Note that 1×10^3 human $CD34^+$ normal BM HSPCs or $CD34^+$ human CML stem/progenitor cells or 5×10^4 primary human BM CML cells were suspended in 100 μL of IMDM with 2% FBS, 0.1% ciportoxin, and 100 U/mL Pen/Strep and added to 1 mL of Methocult H4435 supplemented with 0.1% ciportoxin and 100 U/mL Pen/Strep. DMSO or EZH2 catalytic activity inhibitors were added to the mixture and cell plated onto 35-mm dishes and incubated in 37°C for 9 days before colonies were enumerated.

Statistical Analysis

Statistical analysis was performed by the Student *t* test, unless otherwise indicated. Results were considered significant if the *P* value was < 0.05.

Disclosure of Potential Conflicts of Interest

J.E. Bradner is President, NIBR at Novartis. No potential conflicts of interest were disclosed by the other authors.

Authors' Contributions

Conception and design: H. Xie, C. Peng, W. Kim, S.H. Orkin
Development of methodology: H. Xie, C. Peng, W. Kim, S. Li, S.H. Orkin
Acquisition of data (provided animals, acquired and managed patients, provided facilities, etc.): H. Xie, C. Peng, B.E. Li, E.C. Smith, G. Cheloni, P.P. Das, M. Nguyen, S. Li, S.H. Orkin
Analysis and interpretation of data (e.g., statistical analysis, biostatistics, computational analysis): H. Xie, C. Peng, J. Huang, B.E. Li, P.P. Das, S. Li, J.E. Bradner, S.H. Orkin
Writing, review, and/or revision of the manuscript: H. Xie, C. Peng, J. Qi, P.P. Das, S. Li, J.E. Bradner, S.H. Orkin
Administrative, technical, or material support (i.e., reporting or organizing data, constructing databases): C. Peng, B.E. Li, Y. Fujiwara, J. Qi, J.E. Bradner
Study supervision: H. Xie, C. Peng, S. Li, S.H. Orkin

Acknowledgments

We are grateful to the members of our laboratory for discussions and technical help. We thank Dr. Jerome Ritz and Doreen Hearsey (Dana-Farber Cancer Institute), Dr. Frank C. Kuo (Brigham and Women's Hospital), Dr. Richard Stone, and Ilene Ann Galinsky (Dana-Farber Cancer Institute) for primary CML patient samples.

Grant Support

This work was funded in part by NIH U01 CA105423 (to S.H. Orkin), a Scholar Award from Hyundai Hope on Wheels, and the Harvard Stem Cell Institute Blood Program. H. Xie was a Leukemia and Lymphoma Society fellow. E.C. Smith is supported by a Jane Coffin Childs Memorial Fund for Medical Research Fellowship and a Burroughs Wellcome Fund Postdoctoral Enrichment Program Award.

Received December 7, 2015; revised August 22, 2016; accepted August 25, 2016; published OnlineFirst September 14, 2016.

REFERENCES

1. Nowell PC, Hungerford DA. Chromosome studies on normal and leukemic human leukocytes. J Natl Cancer Inst 1960;25:85–109.
2. Fainstein E, Marcelle C, Rosner A, Canaani E, Gale RP, Dreazen O, et al. A new fused transcript in Philadelphia chromosome positive acute lymphocytic leukaemia. Nature 1987;330:386–8.
3. Ulmer A, Tabea Tauer J, Glauche I, Jung R, Suttorp M. TK inhibitor treatment disrupts growth hormone axis: Clinical observations in children with CML and experimental data from a juvenile animal model. Klin Padiatr 2013;225:120–6.
4. Price KE, Saleem N, Lee G, Steinberg M. Potential of ponatinib to treat chronic myeloid leukemia and acute lymphoblastic leukemia. Onco Targets Ther 2013;6:1111–8.
5. Ahmed W, Van Etten RA. Alternative approaches to eradicating the malignant clone in chronic myeloid leukemia: Tyrosine-kinase inhibitor combinations and beyond. Hematology Am Soc Hematol Educ Program 2013;2013:189–200.
6. Druker BJ, Tamura S, Buchdunger E, Ohno S, Segal GM, Fanning S, et al. Effects of a selective inhibitor of the Abl tyrosine kinase on the growth of Bcr-Abl positive cells. Nat Med 1996;2:561–6.
7. Cortes JE, Kim DW, Pinilla-Ibarz J, le Coutre P, Paquette R, Chuah C, et al. A phase 2 trial of ponatinib in Philadelphia chromosome-positive leukemias. N Engl J Med 2013;369:1783–96.
8. Zabriskie MS, Eide CA, Tantravahi SK, Vellore NA, Estrada J, Nicolini FE, et al. BCR-ABL1 compound mutations combining key kinase domain positions confer clinical resistance to ponatinib in Ph chromosome-positive leukemia. Cancer Cell 2014;26:428–42.

9. Varambally S, Dhanasekaran SM, Zhou M, Barrette TR, Kumar-Sinha C, Sanda MG, et al. The polycomb group protein EZH2 is involved in progression of prostate cancer. Nature 2002;419:624–9.
10. Kleer CG, Cao Q, Varambally S, Shen R, Ota I, Tomlins SA, et al. EZH2 is a marker of aggressive breast cancer and promotes neoplastic transformation of breast epithelial cells. Proc Natl Acad Sci U S A 2003;100:11606–11.
11. Sudo T, Utsunomiya T, Mimori K, Nagahara H, Ogawa K, Inoue H, et al. Clinicopathological significance of EZH2 mRNA expression in patients with hepatocellular carcinoma. Br J Cancer 2005;92:1754–8.
12. Chase A, Cross NC. Aberrations of EZH2 in cancer. Clin Cancer Res 2011;17:2613–8.
13. Raaphorst FM, van Kemenade FJ, Blokzijl T, Fieret E, Hamer KM, Satijn DP, et al. Coexpression of BMI-1 and EZH2 polycomb group genes in Reed-Sternberg cells of Hodgkin's disease. Am J Pathol 2000;157:709–15.
14. Ernst T, Chase AJ, Score J, Hidalgo-Curtis CE, Bryant C, Jones AV, et al. Inactivating mutations of the histone methyltransferase gene EZH2 in myeloid disorders. Nat Genet 2010;42:722–6.
15. Nikoloski G, Langemeijer SM, Kuiper RP, Knops R, Massop M, Tonnissen ER, et al. Somatic mutations of the histone methyltransferase gene EZH2 in myelodysplastic syndromes. Nat Genet 2010;42:665–7.
16. Guglielmelli P, Biamonte F, Score J, Hidalgo-Curtis C, Cervantes F, Maffioli M, et al. EZH2 mutational status predicts poor survival in myelofibrosis. Blood 2011;118:5227–34.
17. Simon C, Chagraoui J, Krosl J, Gendron P, Wilhelm B, Lemieux S, et al. A key role for EZH2 and associated genes in mouse and human adult T-cell acute leukemia. Genes Dev 2012;26:651–6.
18. Neff T, Sinha AU, Kluk MJ, Zhu N, Khattab MH, Stein L, et al. Polycomb repressive complex 2 is required for MLL-AF9 leukemia. Proc Natl Acad Sci U S A 2012;109:5028–33.
19. Wilson BG, Wang X, Shen X, McKenna ES, Lemieux ME, Cho YJ, et al. Epigenetic antagonism between polycomb and SWI/SNF complexes during oncogenic transformation. Cancer Cell 2010;18:316–28.
20. Xie H, Xu J, Hsu JH, Nguyen M, Fujiwara Y, Peng C, et al. Polycomb repressive complex 2 regulates normal hematopoietic stem cell function in a developmental-stage-specific manner. Cell Stem Cell 2014;14:68–80.
21. Cramer-Morales K, Nieborowska-Skorska M, Scheibner K, Padget M, Irvine DA, Sliwinski T, et al. Personalized synthetic lethality induced by targeting RAD52 in leukemias identified by gene mutation and expression profile. Blood 2013;122:1293–304.
22. Subramanian A, Tamayo P, Mootha VK, Mukherjee S, Ebert BL, Gillette MA, et al. Gene set enrichment analysis: A knowledge-based approach for interpreting genome-wide expression profiles. Proc Natl Acad Sci U S A 2005;102:15545–50.
23. Talpaz M, Shah NP, Kantarjian H, Donato N, Nicoll J, Paquette R, et al. Dasatinib in imatinib-resistant Philadelphia chromosome-positive leukemias. N Engl J Med 2006;354:2531–41.
24. Hu Y, Swerdlow S, Duffy TM, Weinmann R, Lee FY, Li S. Targeting multiple kinase pathways in leukemic progenitors and stem cells is essential for improved treatment of Ph+ leukemia in mice. Proc Natl Acad Sci U S A 2006;103:16870–5.
25. Zhang B, Ho YW, Huang Q, Maeda T, Lin A, Lee SU, et al. Altered microenvironmental regulation of leukemic and normal stem cells in chronic myelogenous leukemia. Cancer Cell 2012;21:577–92.
26. Xu K, Wu ZJ, Groner AC, He HH, Cai C, Lis RT, et al. EZH2 oncogenic activity in castration-resistant prostate cancer cells is Polycomb-independent. Science 2012;338:1465–9.
27. Kuzmichev A, Nishioka K, Erdjument-Bromage H, Tempst P, Reinberg D. Histone methyltransferase activity associated with a human multiprotein complex containing the Enhancer of Zeste protein. Genes Dev 2002;16:2893–905.
28. Joshi P, Carrington EA, Wang L, Ketel CS, Miller EL, Jones RS, et al. Dominant alleles identify SET domain residues required for histone methyltransferase of Polycomb repressive complex 2. J Biol Chem 2008;283:27757–66.
29. McCabe MT, Ott HM, Ganji G, Korenchuk S, Thompson C, Van Aller GS, et al. EZH2 inhibition as a therapeutic strategy for lymphoma with EZH2-activating mutations. Nature 2012;492:108–12.
30. Xu B, On DM, Ma A, Parton T, Konze KD, Pattenden SG, et al. Selective inhibition of EZH2 and EZH1 enzymatic activity by a small molecule suppresses MLL-rearranged leukemia. Blood 2015;125:346–57.
31. Konze KD, Ma A, Li F, Barsyte-Lovejoy D, Parton T, Macnevin CJ, et al. An orally bioavailable chemical probe of the lysine methyltransferases EZH2 and EZH1. ACS Chem Biol 2013;8:1324–34.
32. Zhang H, Qi J, Reyes JM, Li L, Rao PK, Li F, et al. Oncogenic deregulation of EZH2 as an opportunity for targeted therapy in lung cancer. Cancer Discov 2016 Jun 16. [Epub ahead of print].
33. Okamura S, Arakawa H, Tanaka T, Nakanishi H, Ng CC, Taya Y, et al. p53DINP1, a p53-inducible gene, regulates p53-dependent apoptosis. Mol Cell 2001;8:85–94.
34. Liu J, Weiss HL, Rychahou P, Jackson LN, Evers BM, Gao T. Loss of PHLPP expression in colon cancer: Role in proliferation and tumorigenesis. Oncogene 2009;28:994–1004.
35. Moulton T, Crenshaw T, Hao Y, Moosikasuwan J, Lin N, Dembitzer F, et al. Epigenetic lesions at the H19 locus in Wilms' tumour patients. Nat Genet 1994;7:440–7.
36. Guan KL, Jenkins CW, Li Y, Nichols MA, Wu X, O'Keefe CL, et al. Growth suppression by p18, a p16INK4/MTS1- and p14INK4B/MTS2-related CDK6 inhibitor, correlates with wild-type pRb function. Genes Dev 1994;8:2939–52.
37. Shi J, Wang E, Milazzo JP, Wang Z, Kinney JB, Vakoc CR. Discovery of cancer drug targets by CRISPR-Cas9 screening of protein domains. Nat Biotechnol 2015;33:661–7.
38. Brinkman EK, Chen T, Amendola M, van Steensel B. Easy quantitative assessment of genome editing by sequence trace decomposition. Nucleic Acids Res 2014;42:e168.
39. Prost S, Relouzat F, Spentchian M, Ouzegdouh Y, Saliba J, Massonnet G, et al. Erosion of the chronic myeloid leukaemia stem cell pool by PPARgamma agonists. Nature 2015;525:380–3.
40. Abraham SA, Hopcroft LE, Carrick E, Drotar ME, Dunn K, Williamson AJ, et al. Dual targeting of p53 and c-MYC selectively eliminates leukaemic stem cells. Nature 2016;534:341–6.
41. Ntziachristos P, Tsirigos A, Van Vlierberghe P, Nedjic J, Trimarchi T, Flaherty MS, et al. Genetic inactivation of the polycomb repressive complex 2 in T cell acute lymphoblastic leukemia. Nat Med 2012;18:298–301.
42. Scott MT, Korfi K, Saffrey P, Hopcroft LEM, Kinstrie R, Pellicano F, et al. Epigenetic reprogramming sensitizes CML stem cells to combined EZH2 and tyrosine kinase inhibition. Cancer Discov 2016;6:1248–57.
43. Srinivas S, Watanabe T, Lin CS, William CM, Tanabe Y, Jessell TM, et al. Cre reporter strains produced by targeted insertion of EYFP and ECFP into the ROSA26 locus. BMC Dev Biol 2001;1:4.
44. Shen X, Liu Y, Hsu YJ, Fujiwara Y, Kim J, Mao X, et al. EZH1 mediates methylation on histone H3 lysine 27 and complements EZH2 in maintaining stem cell identity and executing pluripotency. Mol Cell 2008;32:491–502.
45. Li S, Ilaria RL Jr, Million RP, Daley GQ, Van Etten RA. The P190, P210, and P230 forms of the BCR/ABL oncogene induce a similar chronic myeloid leukemia-like syndrome in mice but have different lymphoid leukemogenic activity. J Exp Med 1999;189:1399–412.